

Climate models struggle to simulate observed North Pacific jet trends, even accounting for tropical Pacific sea surface temperature trends

Article

Published Version

Creative Commons: Attribution 4.0 (CC-BY)

Open Access

Patterson, M. ORCID: <https://orcid.org/0000-0002-9484-8410> and O'Reilly, C. H. ORCID: <https://orcid.org/0000-0002-8630-1650> (2025) Climate models struggle to simulate observed North Pacific jet trends, even accounting for tropical Pacific sea surface temperature trends. *Geophysical Research Letters*, 52 (4). e2024GL113561. ISSN 1944-8007 doi: 10.1029/2024GL113561 Available at <https://centaur.reading.ac.uk/120956/>

It is advisable to refer to the publisher's version if you intend to cite from the work. See [Guidance on citing](#).

To link to this article DOI: <http://dx.doi.org/10.1029/2024GL113561>

Publisher: American Geophysical Union

the [End User Agreement](#).

www.reading.ac.uk/centaur

CentAUR

Central Archive at the University of Reading

Reading's research outputs online



Geophysical Research Letters[®]

RESEARCH LETTER

10.1029/2024GL113561

Key Points:

- The North Pacific jet has shifted northward over the satellite-era but no models show a trend of the same magnitude over this period
- This trend is consistent with variability associated with the Interdecadal Pacific Oscillation and is not necessarily externally forced
- Model-observation differences in tropical Pacific temperature trends can only partially explain differences in North Pacific jet trends

Supporting Information:

Supporting Information may be found in the online version of this article.

Correspondence to:

M. Patterson,
m.r.patterson@reading.ac.uk

Citation:

Patterson, M., & O'Reilly, C. H. (2025). Climate models struggle to simulate observed North Pacific jet trends, even accounting for tropical Pacific sea surface temperature trends. *Geophysical Research Letters*, 52, e2024GL113561. <https://doi.org/10.1029/2024GL113561>

Received 12 NOV 2024

Accepted 2 FEB 2025

Climate Models Struggle to Simulate Observed North Pacific Jet Trends, Even Accounting for Tropical Pacific Sea Surface Temperature Trends

Matthew Patterson¹  and Christopher H. O'Reilly¹

¹Department of Meteorology, University of Reading, Reading, UK

Abstract We show that the wintertime (December–January–February) North Pacific jet in ERA5 has shifted northwards over the satellite-era (1979–2023) at a faster rate than any of the state-of-the-art coupled climate models used in this study. Differences in tropical sea surface temperature (SST) trends can only partially explain the discrepancy in jet trends between models and observations and a small minority of simulations forced with observed SSTs match the magnitude of the observed jet trend. However, analysis of longer-term jet variability in reanalysis suggests that the jet trend has not clearly emerged from multi-decadal internal climate variability. Consequently, it is unclear whether the difference in observed and modeled jet trends arises due to differing responses to anthropogenic forcing or overly weak long-term internal variability in models. These results have important implications for future climate projections for North America and motivate further research into the underlying causes of long-term jet trends.

Plain Language Summary The North Pacific jet stream has a large effect on precipitation and temperatures over North America. Climate model simulations suggest that the jet is likely to move northwards with climate change which could lead to a shift in rainfall patterns. We show that the observed jet has shifted northwards at a faster rate over the past 45 years than in the vast majority of model simulations. However, we cannot rule out the possibility that the observed shift may largely be the result of natural climate variability. Our findings suggest that models either underplay natural jet stream variability or the Pacific jet response to climate change, both of which increase the real uncertainty in future climate change for North America.

1. Introduction

Jet stream variability has a large impact on surface weather variations in the mid-latitudes as well as playing an important role in energy and momentum balances in the atmosphere (Schneider, 2006). In response to increased greenhouse gas concentrations, idealized and comprehensive climate models generally simulate a poleward shift of the zonal mean jets in both hemispheres (e.g., Barnes & Polvani, 2013; Butler et al., 2010; Patterson et al., 2019; Rivière, 2011; Simpson et al., 2014), though the precise mechanism governing these shifts is the subject of considerable debate (Shaw, 2019). Projections of jet shifts also vary regionally and by season (Ossó et al., 2024; Simpson et al., 2014) with some models showing an equatorward shift of the North and South Pacific jet exit regions under weak future warming scenarios (Li et al., 2018). Any jet shifts would significantly affect regional precipitation, for example, and future jet changes constitute a major source of uncertainty in future regional climate change projections (e.g., Harvey et al., 2023; Mindlin et al., 2020; Zappa & Shepherd, 2017).

Recent observational studies have shown evidence for statistically significant poleward shifts in the wintertime northern hemisphere zonal mean jet (Woollings et al., 2023) and North Pacific jet (Keel et al., 2024) over the satellite era (1979–present). However, this is a short enough period that internal modes of climate variability, such as the Interdecadal Pacific Oscillation (IPO, e.g. Henley et al., 2015) or Atlantic Multidecadal Variability (e.g., Zhang et al., 2019), may influence these trends.

Furthermore, observed sea surface temperature (SST) trends from around 1960 to present in the tropical Pacific are inconsistent with trends simulated by climate models (Coats & Karnauskas, 2017; Seager et al., 2019, 2022). Specifically, the observed trend consists of cooling along the equator whereas models tend to warm (Seager et al., 2019). There remains debate over whether this discrepancy is a forced response to climate change which isn't captured by models (Seager et al., 2019), a manifestation of internal variability (Chung et al., 2019; Watanabe

© 2025. The Author(s).

This is an open access article under the terms of the [Creative Commons](#)

[Attribution License](#), which permits use, distribution and reproduction in any medium, provided the original work is properly cited.

et al., 2021; Wu et al., 2021) or a combination of these two (Heede & Fedorov, 2023; Rugenstein et al., 2023; Wills et al., 2022).

Regardless of the drivers of this discrepancy, tropical Pacific SST variability has global impacts via atmospheric teleconnections (Trenberth et al., 1998) and is hence, highly likely to have a substantial impact on trends in atmospheric circulation. In this study, we examine trends in the wintertime North Pacific jet in reanalysis and models from the Coupled Model Intercomparison Project Phase 6 (Eyring et al., 2016) and investigate the impact that tropical Pacific SSTs have on these trends.

2. Data and Methods

2.1. Model and Reanalysis Data

We analyze monthly mean zonal wind and SST data from the Coupled Model Intercomparison Project Phase 6 (Eyring et al., 2016). Specifically, we combine historical simulations with corresponding simulations for the scenario run, “shared socioeconomic pathway 585” (ssp585; Meinshausen et al., 2020), to create a time series spanning 1979–2023. These simulations are forced by specified variations in greenhouse gases and aerosols as well as other forcings such as volcanic and solar radiation. We use up to 10 members for each model so that models with a large number of members do not dominate the results, however the results are essentially unchanged if all available members are used (e.g., Supplementary Figure S2 in Supporting Information S1). Only simulations for which both historical and ssp585 data are available are analyzed. We also analyze atmosphere-only simulations from corresponding atmospheric model intercomparison project (AMIP) simulations and atmosphere-only simulations from the experiment ‘highresSST-present’ within the HighResMip project (Haarsma et al., 2016). A full list of model simulations analyzed is given in Supplementary Tables S1 and S2 in Supporting Information S1.

For observation-based data sets, we use monthly mean HadISST SSTs (Rayner et al., 2003; Titchner & Rayner, 2014) and monthly mean precipitation data from the Global Precipitation Climatology Project (GPCP, Adler et al., 2018), Climate Research Unit (CRU) multivariate climate data set (Harris et al., 2020) and the Climate Hazards InfraRed Precipitation with Station data data set (CHIRPS, Funk et al., 2015). We also use monthly mean zonal wind from four reanalysis data sets; modern data sets ERA5 (1940–2023, Hersbach et al., 2020) and JRA-55 (1958–2023, Kobayashi et al., 2015) and two spanning the twentieth century, ERA-20C (1900–2010, Poli et al., 2016) and 20th Century Reanalysis version 3 (1836–2015, L. C. Slivinski et al., 2021). The modern data sets utilize the full range of available observations including satellite observations, whereas the longer data sets only assimilate surface winds and sea level pressure and so are less well constrained by observations.

2.2. Jet Latitude Indices

Many jet indices, particularly for the North Atlantic and southern hemisphere, have used lower level (often 850 hPa) winds to isolate the eddy-driven portion of the flow (e.g., Woollings et al., 2010). This also has the advantage of being more closely correlated with surface weather. However, variability of the North Pacific jet is more thermally driven (Li & Wettstein, 2012) and the lower level winds are largely controlled by this upper tropospheric variability. We therefore primarily analyze 250 hPa zonal winds. Specifically, we calculate a jet index, based on the method of Bracegirdle et al. (2018) but for the 250 hPa level, in which the seasonal-mean zonal mean zonal wind, is calculated within the North Pacific sector (140°E–120°W, 20°N–70°N) and interpolated using a cubic spline onto a resolution of 0.1°. The jet latitude is then the latitude of the maximum North Pacific sector zonal mean zonal wind for the December–January–February (DJF) season. To test the sensitivity to the jet latitude index, we calculate a jet index following Zappa et al. (2018) as the mean latitude, weighted by the square of the 850 hPa zonal wind, where the wind is westerly, averaged over the same North Pacific sector. That is,

$$\phi_{jet} = \int_{20^\circ}^{70^\circ} u_0^2 \phi \, d\phi / \int_{20^\circ}^{70^\circ} u_0^2 \, d\phi \quad (1)$$

where ϕ is the latitude and u_0 is the North Pacific sector zonal mean zonal wind, but with u_0 being zero where the wind is easterly. For the majority of this paper, the index based on Bracegirdle et al. (2018) is used.

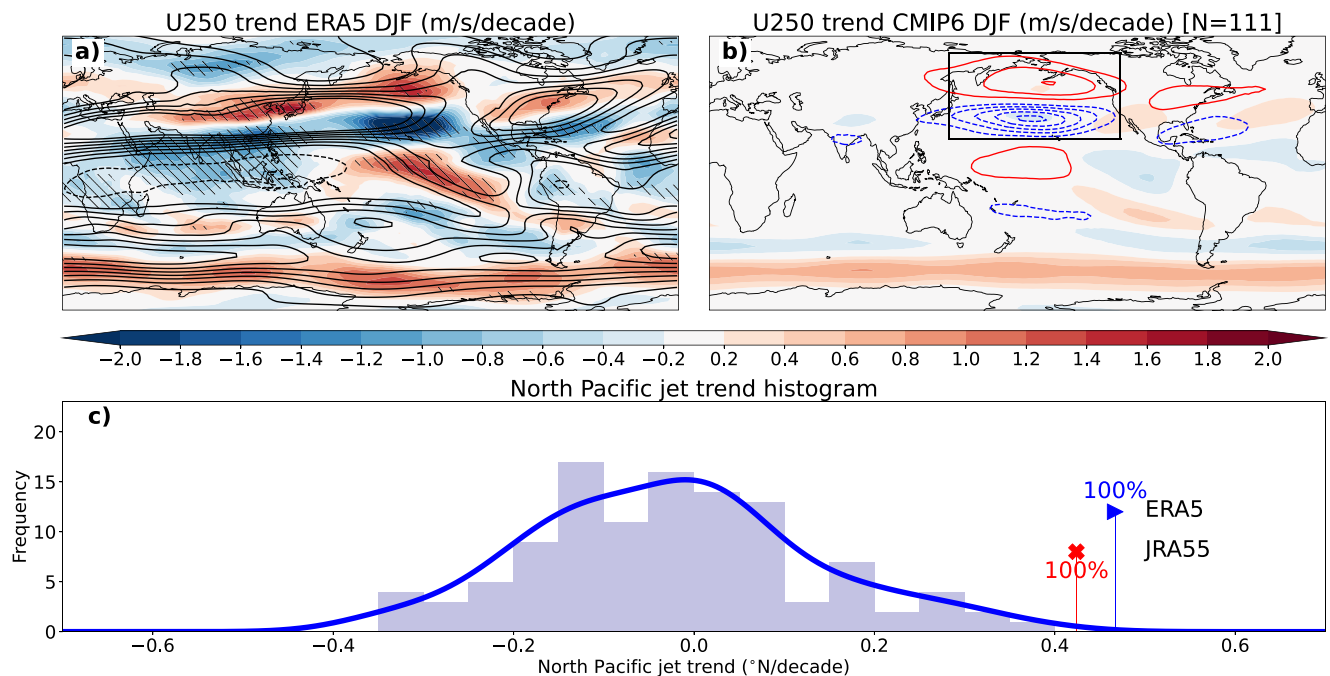


Figure 1. Trends in the DJF North Pacific jet in models and observations (1979–2023). (a) The trend in ERA5 250 hPa zonal wind is shown by filled colors with the climatology indicated by unfilled contours, drawn every 10 m/s. Hatching in (a) indicates the grid-points at which the ERA5 trend lies outside of the middle 95% of the ensemble of model trends. (b) The mean of 250 hPa zonal wind trends for all CMIP6 ensemble members (filled colors) and the leading EOF of model trends across all members within the North Pacific region (unfilled contours, red for positive and blue for negative values, contoured at intervals of 1 m/s/decade/σ). The North Pacific region is shown by a box in (b). The distribution of model jet latitude trends is shown in (c), with ERA5 and JRA-55 jet trends shown by a triangle and a cross, respectively. In this and subsequent figures, percentages adjacent to symbols indicate the percentile at which these lie with respect to the CMIP6 distribution.

3. Results

3.1. Observed and Modeled North Pacific Jet Trends

We begin by comparing wintertime (December–January–February, DJF), upper-tropospheric zonal wind trends in models and ERA5 over the satellite era (1979–2023). Consistent with Keel et al. (2024) there is a northward shift of the jet over the North Pacific (Figure 1a). This shift is strongest over the eastern North Pacific, though there is also a strengthening of the jet on the poleward flank near Japan (Figure 1a). The jet has weakened markedly on the equatorward flank, downstream of the main jet core (Figure 1a). Intriguingly, this jet shift pattern is not present in the CMIP6 mean (Figure 1b). It should be noted that averaging over many CMIP6 simulations hides a range of different behaviors. The leading empirical orthogonal function (EOF) of zonal wind trend maps over the North Pacific sector over all ensemble members, is a meridional jet shift, explaining 46% of the variance in trends across the CMIP6 ensemble (Figure 1b). Nevertheless, the North Pacific zonal wind trends in ERA5 lie outside of the middle 95% of the model trend ensemble (Figure 1a). Notably, the ERA5 zonal winds trends over East Asia also lie outside of the middle 95% of model trends (Figure 1a).

To visualize the spread of North Pacific jet trends in models we calculate a jet latitude index (see the materials and methods section) for each model and calculate the trend. The ERA5 and JRA-55 jet trends of 0.47°N/decade and 0.43°N/decade lie outside of the model spread (Figure 1c). For Figures 1b and 1c only up to 10 ensemble members are taken from each model so that models with many members do not dominate, however the figure is almost identical when all available members are plotted (Supplementary Figure S1 in Supporting Information S1). If the jet latitude index is evaluated on the 850 hPa level rather than at 250 hPa, the ERA5 and JRA-55 reanalysis trends are 0.69°N/decade and 0.71°N/decade, respectively (Supplementary Figure S2c in Supporting Information S1). In this case, 5 and 4 simulations out of 180 exceed the ERA5 and JRA-55 trends, respectively (Supplementary Figure S2c in Supporting Information S1). The study of Keel et al. (2024) noted that the choice of jet detection method was a larger source of uncertainty than the reanalysis data set in North Pacific jet trends. However, calculating the jet latitude index using the method of Zappa et al. (2018) on 850 hPa gives similar results to the original index,

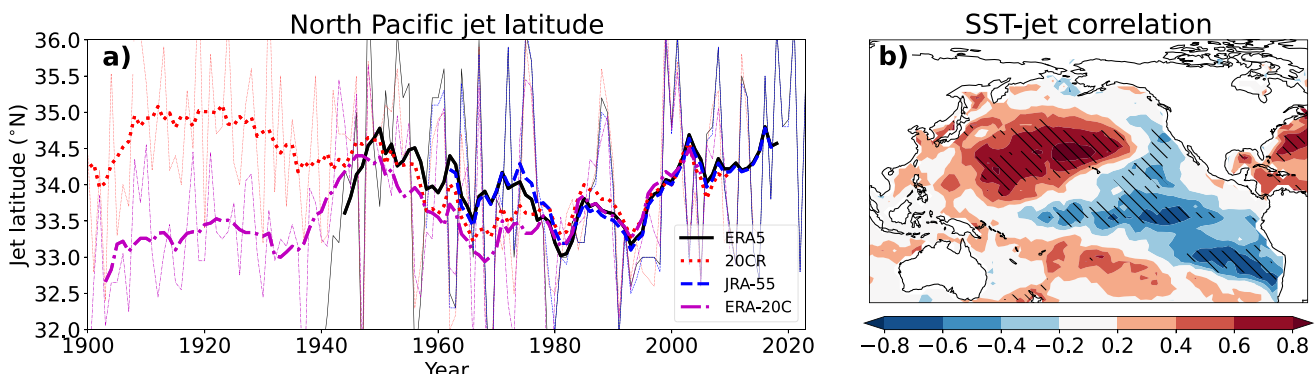


Figure 2. (a) Jet latitude time series constructed from four different reanalysis data sets. Interannual variability is shown by thin lines and the 10 years running mean for each time series is shown by a thicker line. (b) Map showing the correlation between the 10 years running mean ERA5 jet and HadISST time series at each grid-point (1940–2023). Hatching indicates where grid-point correlations have p -values below 0.05, following the phase-shuffling method of Ebisuzaki (1997).

with the reanalysis trends exceeding trends in almost all model simulations (Supplementary Figure S3 in Supporting Information S1). In summary, the greater northward jet trend in observations relative to models is not sensitive to the choice of methodology.

The observed northward North Pacific jet trend has important implications for regional precipitation change. All three precipitation data sets analyzed show a clear drying trend for the southern US and Mexico over the satellite-era which is not captured by the CMIP6 ensemble-mean (Supplementary Figures S4a–S4d in Supporting Information S1). However, the 10% of model simulations with the most northward jet trends do simulate the drying trend, underlining the role of dynamics in recent precipitation trends (Supplementary Figure S4e in Supporting Information S1). There is, however, some disagreement amongst data sets on whether or not there has been a wetting trend further north along the coast around Washington State and British Columbia, like that seen in the CMIP6 models (Supplementary Figures S4a–S4c and S4e in Supporting Information S1).

To put the jet trend into a longer term context, we plot reanalysis estimates of variations in the 250 hPa jet latitude index throughout the twentieth century (Figure 2a). There is good consistency in the low-frequency variability of the jet in the reanalyses back to around 1950. Before this the data sets diverge, likely because of the underlying dynamical models reverting to their mean states due to a paucity of observations (Figure 2a). Hence, we focus on jet variability in the period from 1950 onwards. Post-1950, there is clear multi-decadal variability in the jet latitude with a southward trend until around 1980. Following this, the jet shifts northward after 1980, hence the northward shift coincides with the beginning of the satellite-era. These low-frequency variations in jet variability are strongly correlated with a pattern of SST variations which resembles the IPO, with positive anomalies in the extratropical North Pacific and negative anomalies in the tropics (Figure 2b). The link between low-frequency Pacific SST variability and North Pacific atmospheric circulation is well established (e.g., Dai, 2013; Patterson et al., 2022; Robertson, 1996; Trenberth & Hurrell, 1994). Tropical SSTs are thought to influence the North Pacific jet via Rossby wave dynamics, while the jet alters extratropical SST by modulating the air-sea heat flux (Newman et al., 2016). However, there is also some evidence of a weak effect of extratropical atmospheric circulation on tropical SSTs (Dow et al., 2024). Overall, Figure 2 makes it clear that recent trends in the North Pacific jet have not clearly emerged from long-term internal variability, however it is possible that external forcing has contributed to the recent jet trend.

3.2. The Role of Tropical Pacific SST Variability

Noting the discrepancy between modeled and observed trends (Figure 1) and the link between observed North Pacific jet variability and Pacific SSTs (Figure 2b; Trenberth & Hurrell, 1994; Robertson, 1996) we now investigate the degree to which differences in tropical Pacific SST trends can explain the jet trend discrepancy. Since the beginning of the satellite-era in 1979, the tropical Pacific in DJF has cooled, in contrast to the broader global warming trend (Figure 3a). On the other hand, the tropical Pacific has generally warmed in CMIP6 simulations covering this same period (Figure 3b) and the observations lie at the tail of the simulated trends (Figure 3a). On an interannual basis, a northward shift of the North Pacific jet is generally associated with a

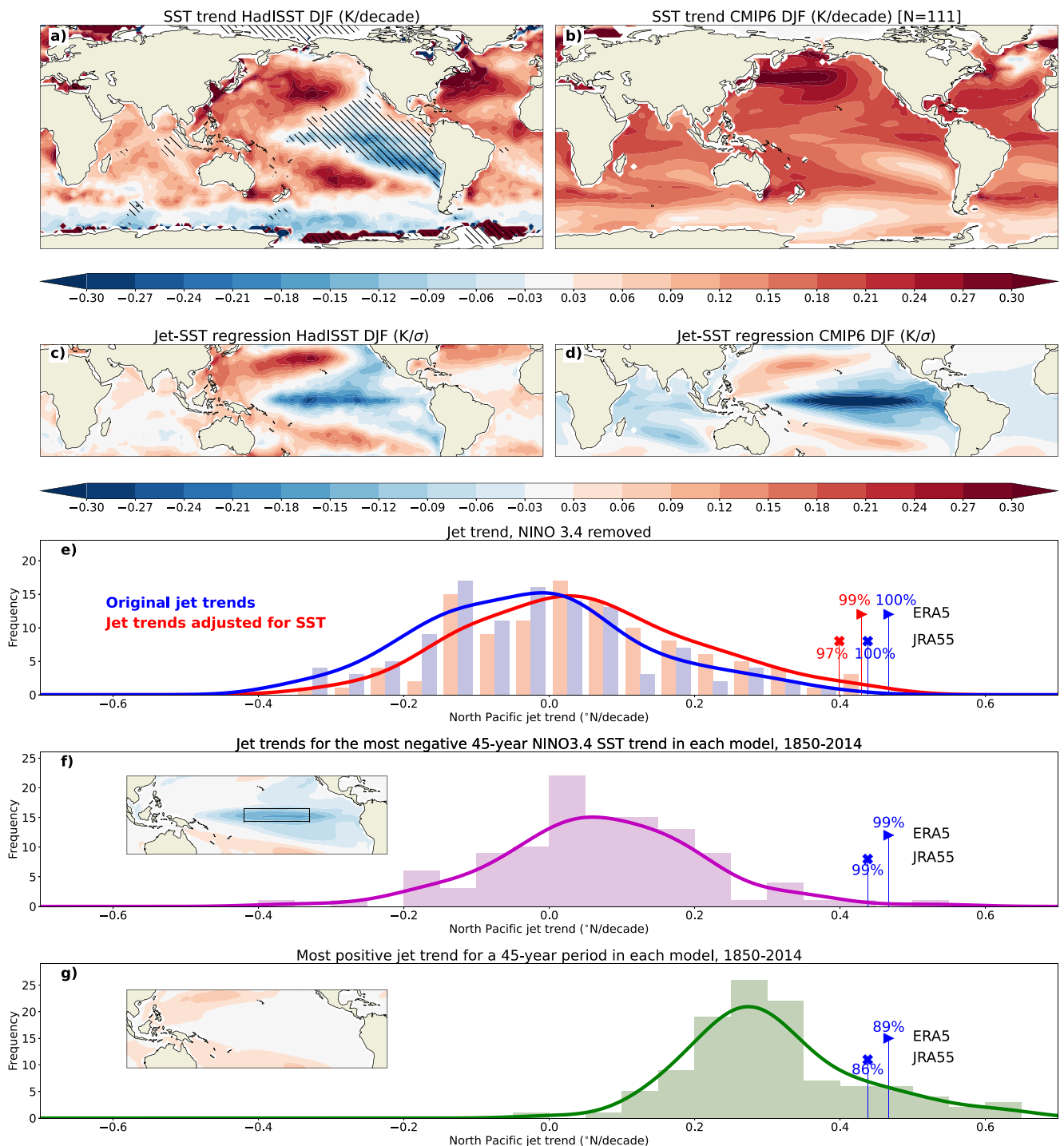


Figure 3. Trends in SSTs (DJF, 1979–2023) and their impact on the North Pacific jet trend. The trend is shown for (a) HadISST (b) the mean over trends in all CMIP6 members. Hatching in (a) indicates grid-points at which HadISST trends lie outside of the middle 95% of the CMIP6 ensemble. The regression of the SSTs onto jet index is shown for (c) HadISST/ERA5 and (d) the mean over CMIP6 members. Jet trend distributions are shown (e) before (blue) and after (red) linearly removing the Niño 3.4 index, (f) the period with the most negative Niño 3.4 SST trends in the historical simulations for each simulation and (g) the period with the largest jet trend in each simulation. Distributions in (e)–(g) are shown by histograms with a distribution function calculated from a Gaussian kernel density estimate; the percentiles of the ERA5 trend with respect to the different CMIP6 distributions are also shown. Inset panels in (f), (g) show the SST trends over the corresponding periods, averaged across all simulations, using the same contour interval and units as panels (a), (b). The box in the inset panel in (f) shows the Niño 3.4 region.

cooling of the tropical Pacific in both observations (Figure 3c) and models (Figure 3d), therefore the cooling trend in observations may have contributed to the northward jet trend.

To assess the role of the cooling trend, we linearly remove the Niño 3.4 index (SST averaged over 170°W–120°W, 5°S–5°N) from the jet latitude index for each model member and for observations, and calculate the new trend. The results are insensitive to the use of other El Niño Southern Oscillation (ENSO) indices (Supplementary Figure S5 in Supporting Information S1) or using a more complex method to remove the optimal SST-jet teleconnection pattern from the jet time series (Supplementary Figure S6 in Supporting Information S1). Regressing out the tropical SST influence reduces the ERA5 and JRA55 jet trends from 0.47°N/decade and 0.43°N/decade to 0.42°N/decade and 0.4°N/decade, respectively, and shifts the ensemble of CMIP6 simulations (Figure 3e). Nevertheless, ERA5/JRA55 remain at the tail of the CMIP6 distribution (99th and 97th percentiles, Figure 3e) suggesting that this can explain some but not all of the discrepancy. When the Niño 3.4 index is linearly removed from zonal wind variability at each grid-point, trend maps also show ERA5 lying near the edge of the CMIP6 distribution (Supplementary Figure S7 in Supporting Information S1).

To further examine the role of the tropical Pacific cooling, we find the period with the most negative DJF Niño 3.4 trend over a 45-year period in each historical simulation (1850–2014) and plot a histogram of the corresponding jet trends. The inset panel in Figure 3f shows the mean of the most negative Niño 3.4 trends, which approximately resembles the observations in magnitude and pattern (Figure 3a). The jet trends corresponding to these analogue periods are more northward (Figure 3f) than for the same simulations in the recent period (Figure 3e). However, only one analogue SST period shows a northward jet trend of a greater magnitude than ERA5 (Figure 3f). To illustrate how extreme the ERA5/JRA55 trends are relative to the models, we plot a histogram of the highest 45-year trend measured across the period of the historical experiment (1850–2014) for each simulation (Figure 3g). The ERA5 and JRA55 jet trends lie at the 89th and 86th percentiles compared to these maximum jet trends, respectively. This is not a particularly fair comparison given that the 1979–2023 period has not been cherry picked and we do not have accurate jet time series stretching back to 1850 to find the maximum trend in observations. This analysis suggests that unless the recent period is extremely unusual, the models struggle to capture the strength of jet trends seen in observations. Note that the inset panel in Figure 3g shows these strong positive jet trends tend to occur when the eastern tropical Pacific is warming less than more western and subtropical regions, a negative IPO-like pattern. Nevertheless, the SST trends can only explain part of these jet trends.

We further analyze the role of SST trends in North Pacific jet trends using atmosphere-only simulations forced with observed SSTs. We compare the atmosphere-only models with observations over the period 1979–2014 as AMIP and highresSST-present simulations end in 2014. Atmospheric model intercomparison project simulations show a northward jet trend over this period (Figure 4b), similar to ERA5 and also capture the pattern of the circulation trend over East Asia (Figure 4a). This clearly shows that the SSTs do contribute to the observed trend. However, the ERA5 trend still is larger than most model trends (Figure 4a). Moreover, plotting the histogram of jet trends shows that the ERA5 and JRA55 jet trends are more northward than 97% and 89% of model trends, respectively (Figure 4e).

The resolution of coupled climate models is limited, for practical reasons, but it is of interest to examine how these jet trends might vary in higher resolution models. We test the role of resolution by selecting groups of high and low resolution models from the HighResMIP project (Haarsma et al., 2016). Specifically, we choose all models which have performed both high and low resolution simulations for the highresSST-present experiment (which is broadly similar to the AMIP protocol), giving 13 and 18 ensemble members for the high and low resolution groups, respectively, from a total of 6 model ‘families’. The full lists of models in each group are given in Supplementary Table S2 in Supporting Information S1. Note that we test whether the trends are statistically significantly different by creating 1,000 sets of synthetic composites by randomly shuffling the HighResMIP members between the two composite groups and calculating the difference in the means of these synthetic composites. Differences are deemed statistically significantly different at the 5% level for a given grid-point if the absolute value of the true high-low composite difference is larger than at least 95% of the synthetic composite differences. The high and low resolution models show a very similar trend (Figures 4c and 4d) and these models do not clearly show an improvement on the full AMIP ensemble (Figure 4e). It therefore appears that factors beyond atmospheric resolution are important for capturing the observed North Pacific jet trend or that much higher resolutions are required to see an improvement.

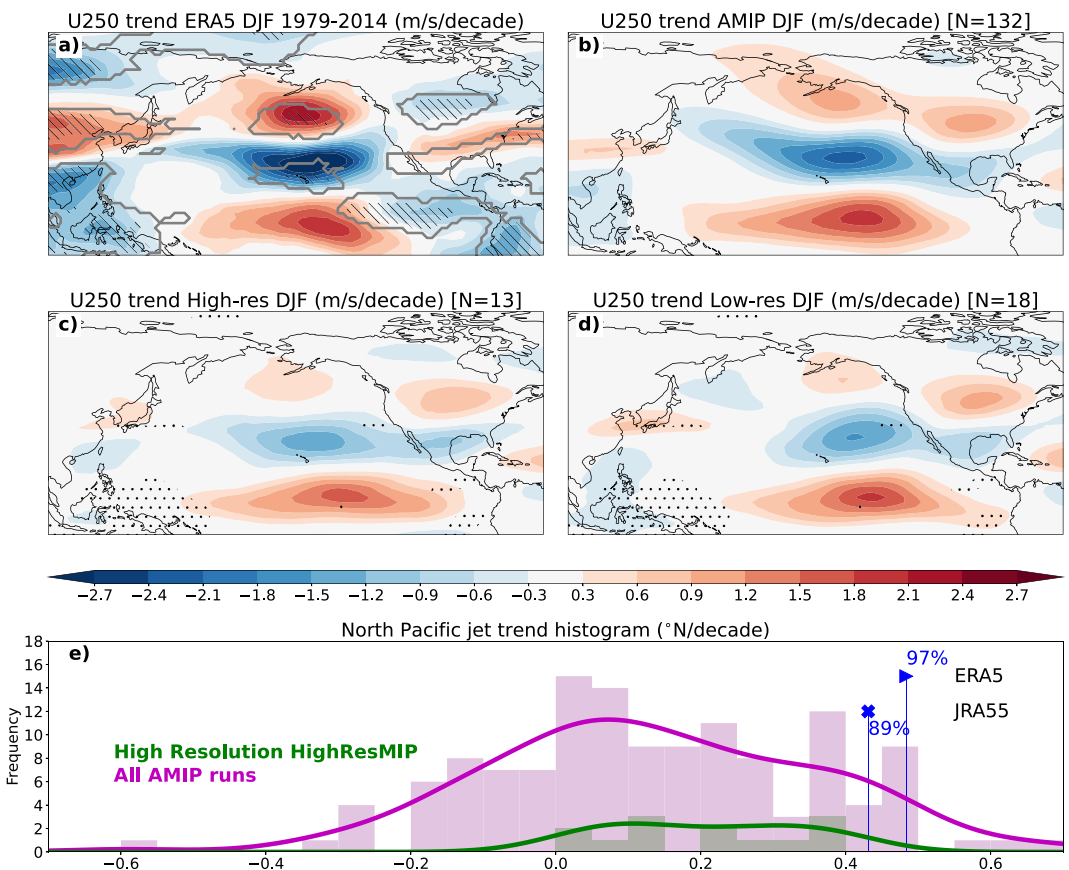


Figure 4. Trends in 250 hPa zonal wind in atmospheric model intercomparison project (AMIP) simulations (DJF, 1979–2014). (a) The trend in ERA5 and (b) the mean of the trends in all AMIP members, (c) the mean of trends in high resolution highresSST-present members and (d) the mean of trends in low resolution highresSST-present members. Hatching and gray contours in (a) indicate grid-points where ERA5 lies outside of the middle 95% and middle 80% of the AMIP distribution, respectively, and stippling in (c), (d) indicates where the high and low resolution groups are statistically significantly different at the 5% level, calculated via a shuffling method (see text). In (e), histograms of the jet trends from the AMIP (magenta) and high resolution (green) models are shown, with ERA5 shown by a triangle and JRA55 by a cross.

4. Summary and Discussion

Over the past 45 years, the wintertime North Pacific jet has shifted northwards (Figures 1a–1c). The magnitude of this trend exceeds all coupled model simulations studied (Figure 1c). However, analysis of longer-term jet variability in reanalysis data sets suggests that the observed trend could be mostly a manifestation of internal climate variability (Figure 2), rather than a purely anthropogenically forced trend. Previous work has shown that observed cooling trends in tropical Pacific sea surface temperatures (SSTs) are inconsistent with recent generations of coupled general circulation models, which mainly show a warming (e.g., Seager et al., 2022). If this is accounted for, the observed jet trend lies within the spread of coupled model trends, but still at the upper end (Figure 3e). Indeed, the ERA5 and JRA55 North Pacific jet trends over the 1979–2023 period are larger than the largest 45-year period jet trend in 89% and 86% of all model historical simulations over the 1850–2014 period, respectively (Figure 3g). Atmosphere-only simulations corroborate this picture. Imposing the observed SSTs leads to a northward shift in the mean of the simulations (Figure 4b), but only a small minority of models show a similar or larger magnitude of North Pacific jet trend relative to ERA5 (Figure 4e). Overall, this suggests that while SST trends play a substantial role in the observed North Pacific jet trend, this cannot account for the larger trend in observations relative to models.

These results clearly have implications for future projections. North Pacific jet variability has a large impact on temperatures and precipitation for the US and Canada. The inability of models to capture observed tropical Pacific SST trends over the past 60 years means that there is considerable uncertainty concerning the accuracy of those

same models' future projections of tropical Pacific SSTs. The teleconnection between the tropical Pacific Ocean and the North Pacific jet implies that we should therefore be less confident in future jet projections, introducing uncertainties around future surface weather over North America.

Moreover, the weaker jet trends in models relative to observations, even accounting for differing SST trends, introduces a further uncertainty in the ability of models to capture future jet trends. There may be a number of reasons for this discrepancy, though assessing these is beyond the scope of this article. One hypothesis surrounds the weaker interannual ENSO teleconnections in many models relative to observations (e.g., Williams et al., 2023), however the jet teleconnection does not appear to be systematically too weak in the AMIP models (Supplementary Figure S8 in Supporting Information S1). A more subtle possibility is that ocean-atmosphere coupling in the extratropical North Pacific acts as a positive feedback, on atmospheric circulation anomalies forced from the tropics, on multi-decadal time-scales. This would explain why removing the interannual ENSO teleconnection in Figure 3e), does not resolve the jet trend difference. Furthermore, an overly weak jet trend has also been noted for the wintertime North Atlantic (Blackport & Fyfe, 2022). The authors of that study also posited that overly weak extratropical ocean-atmosphere interactions in the North Atlantic (Simpson et al., 2018) could be responsible for the weak jet trends, while others have shown that multi-decadal variability is too weak for the North Atlantic (Eade et al., 2024; O'Reilly et al., 2021).

Finally, differing responses to external forcings (such as aerosols), in models and observations, could also be a factor in their differing jet trends. This study cautions against attributing observed North Pacific jet trends to anthropogenic climate change. However, it does not preclude the possibility that aerosols or greenhouse gases have contributed to the recent North Pacific jet trend, either via tropical SSTs or more directly, by altering tropospheric meridional temperature gradients (e.g., Woollings et al., 2023).

It is clear that further research is required to investigate the drivers of observed North Pacific jet trends and to assess the degree to which anthropogenic forcing may have contributed. Moreover, the weaker jet trends in models relative to observations presents an important puzzle to unravel, in order to improve model future projections for the North Pacific region.

Data Availability Statement

No new data were created as part of this study. ERA5 data are available from the Climate Data Store Copernicus Climate Change Service (2019) at <https://doi.org/10.24381/cds.6860a573> and JRA-55 JMA/Japan (2013) at <https://doi.org/10.5065/D60G3H5B>, 20th Century Reanalysis L. L. Slivinski (2019) at <https://doi.org/10.5065/H93G-WS83>, and ERA-20C ECMWF (2014) at <https://doi.org/10.5065/D6VQ30QG> are all available from the NCAR website. HadISST data can be downloaded from the Met Office website at <https://www.metoffice.gov.uk/hadobs/hadisst/data/download.html>, CRU data from the Centre for Environmental Data Analysis site at <https://catalogue.ceda.ac.uk/uuid/5fda109ab71947b6b7724077bf7eb753/>, GPCP data from the NOAA website at <https://downloads.psl.noaa.gov/Datasets/gpcp/> and CHIRPS at <https://www.chc.ucsb.edu/data>. Finally, CMIP6 data, including for the historical, ssp585, AMIP and HighResMIP experiments, are available from the Earth System Grid Federation (ESGF) servers at <https://esgf-ui.ceda.ac.uk/cog/search/cmip6-ceda/>.

Acknowledgments

The authors were both funded through the Royal Society, grant number (URF/R1/201230). We acknowledge the World Climate Research Programme, which, through its Working Group on Coupled Modelling, coordinated and promoted CMIP6. We thank the climate modelling groups for producing and making available their model output, the ESGF for archiving the data and providing access, and the multiple funding agencies who support CMIP6 and ESGF. We also thank two anonymous reviewers, whose thoughtful comments helped us to clarify several important aspects of the paper.

References

- Adler, R. F., Sapiro, M., Huffman, G. J., Wang, J., Gu, G., Bolvin, D., et al. (2018). The global precipitation climatology project (GPCP) monthly analysis (new version 2.3) and a review of 2017 global precipitation. *Atmosphere*, 9(4), 138. <https://doi.org/10.3390/atmos9040138>
- Barnes, E. A., & Polvani, L. (2013). Response of the midlatitude jets, and of their variability, to increased greenhouse gases in the CMIP5 models. *Journal of Climate*, 26(18), 7117–7135. <https://doi.org/10.1175/JCLI-D-12-00536.1>
- Blackport, R., & Fyfe, J. C. (2022). Climate models fail to capture strengthening wintertime North Atlantic jet and impacts on Europe. *Science Advances*, 8(45), eabn3112. <https://doi.org/10.1126/sciadv.abn3112>
- Bracegirdle, T. J., Lu, H., Eade, R., & Woollings, T. (2018). Do CMIP5 models reproduce observed low-frequency North Atlantic jet variability? *Geophysical Research Letters*, 45(14), 7204–7212. <https://doi.org/10.1029/2018GL078965>
- Butler, A. H., Thompson, D. W. J., & Heikes, R. (2010). The steady-state atmospheric circulation response to climate change-like thermal forcings in a simple general circulation model. *Journal of Climate*, 23(13), 3474–3496. <https://doi.org/10.1175/2010JCLI3228.1>
- Chung, E.-S., Timmermann, A., Soden, B. J., Ha, K.-J., Shi, L., & John, V. O. (2019). Reconciling opposing Walker circulation trends in observations and model projections. *Nature Climate Change*, 9(5), 405–412. <https://doi.org/10.1038/s41558-019-0446-4>
- Coats, S., & Karinauskas, K. B. (2017). Are simulated and observed twentieth century tropical Pacific sea surface temperature trends significant relative to internal variability? *Geophysical Research Letters*, 44(19), 9928–9937. <https://doi.org/10.1002/2017GL074622>
- Copernicus Climate Change Service. (2019). ERA5 monthly averaged data on pressure levels from 1940 to present. *Copernicus Climate Change Service (C3S) Climate Data Store (CDS)*. [Dataset]. <https://doi.org/10.24381/CDS.6860A573>

Dai, A. (2013). The influence of the inter-decadal Pacific oscillation on US precipitation during 1923–2010. *Climate Dynamics*, 41(3), 633–646. <https://doi.org/10.1007/s00382-012-1446-5>

Dow, W. J., McKenna, C. M., Joshi, M. M., Blaker, A. T., Rigby, R., & Maycock, A. C. (2024). Sustained intensification of the Aleutian Low induces weak tropical Pacific sea surface warming. *Weather and Climate Dynamics*, 5(1), 357–367. <https://doi.org/10.5194/wcd-5-357-2024>

Eade, R., Stephenson, D. B., Scaife, A. A., & Smith, D. M. (2024). Recalibration of missing low-frequency variability and trends in the North Atlantic Oscillation. *Climate Dynamics*, 62(8), 7869–7887. <https://doi.org/10.1007/s00382-024-07311-1>

Ebisuzaki, W. (1997). A method to estimate the statistical significance of a correlation when the data are serially correlated. *Journal of Climate*, 10(9), 2147–2153. [https://doi.org/10.1175/1520-0442\(1997\)010<2147:AMTETS>2.0.CO;2](https://doi.org/10.1175/1520-0442(1997)010<2147:AMTETS>2.0.CO;2)

ECMWF. (2014). ERA-20C project (ECMWF atmospheric reanalysis of the 20th century). *Research Data Archive at the National Center for Atmospheric Research, Computational and Information Systems Laboratory*. [Dataset]. <https://doi.org/10.5065/D6VQ30QG>

Eyring, V., Bony, S., Meehl, G. A., Senior, C. A., Stevens, B., Stouffer, R. J., & Taylor, K. E. (2016). Overview of the coupled model inter-comparison project phase 6 (CMIP6) experimental design and organization. *Geoscientific Model Development*, 9(5), 1937–1958. <https://doi.org/10.5194/gmd-9-1937-2016>

Funk, C., Peterson, P., Landsfeld, M., Pedreros, D., Verdin, J., Shukla, S., et al. (2015). The climate hazards infrared precipitation with stations—A new environmental record for monitoring extremes. *Scientific Data*, 2(1), 150066. <https://doi.org/10.1038/sdata.2015.66>

Haarsma, R. J., Roberts, M. J., Vidale, P. L., Senior, C. A., Bellucci, A., Bao, Q., et al. (2016). High resolution model intercomparison project (HighResMIP v1.0) for CMIP6. *Geoscientific Model Development*, 9(11), 4185–4208. <https://doi.org/10.5194/gmd-9-4185-2016>

Harris, I., Osborn, T. J., Jones, P., & Lister, D. (2020). Version 4 of the CRU TS monthly high-resolution gridded multivariate climate dataset. *Scientific Data*, 7(1), 109. <https://doi.org/10.1038/s41597-020-0453-3>

Harvey, B., Hawkins, E., & Sutton, R. (2023). Storylines for future changes of the North Atlantic jet and associated impacts on the UK. *International Journal of Climatology*, 43(10), 4424–4441. <https://doi.org/10.1002/joc.8095>

Heede, U. K., & Fedorov, A. V. (2023). Colder eastern equatorial Pacific and stronger walker circulation in the early 21st century: Separating the forced response to global warming from natural variability. *Geophysical Research Letters*, 50(3), e2022GL101020. <https://doi.org/10.1029/2022GL101020>

Henley, B. J., Gergis, J., Karoly, D. J., Power, S., Kennedy, J., & Folland, C. K. (2015). A tripole index for the interdecadal Pacific oscillation. *Climate Dynamics*, 45(11), 3077–3090. <https://doi.org/10.1007/s00382-015-2525-1>

Hersbach, H., Bell, B., Berrisford, P., Hirahara, S., Horányi, A., Muñoz-Sabater, J., et al. (2020). The ERA5 global reanalysis. *Quarterly Journal of the Royal Meteorological Society*, 146(730), 1999–2049. <https://doi.org/10.1002/qj.3803>

JMA/Japan. (2013). JRA-55: Japanese 55-year reanalysis, monthly means and variances. *Research Data Archive at the National Center for Atmospheric Research, Computational and Information Systems Laboratory*. [Dataset]. <https://doi.org/10.5065/D60G3H5B>

Keel, T., Brierley, C., Edwards, T., & Frame, T. H. A. (2024). Exploring uncertainty of trends in the North Pacific jet position. *Geophysical Research Letters*, 51(16), e2024GL109500. <https://doi.org/10.1029/2024GL109500>

Kobayashi, S., Ota, Y., Harada, Y., Ebina, A., Moriya, M., Onoda, H., et al. (2015). The JRA-55 reanalysis: General specifications and basic characteristics. *Journal of the Meteorological Society of Japan*, 93(1), 5–48. <https://doi.org/10.2151/jmsj.2015-001>

Li, C., Michel, C., Seland Graff, L., Bethke, I., Zappa, G., Bracegirdle, T. J., et al. (2018). Midlatitude atmospheric circulation responses under 1.5 and 2.0°C warming and implications for regional impacts. *Earth System Dynamics*, 9(2), 359–382. <https://doi.org/10.5194/esd-9-359-2018>

Li, C., & Wettstein, J. J. (2012). Thermally driven and eddy-driven jet variability in reanalysis. *Journal of Climate*, 25(5), 1587–1596. <https://doi.org/10.1175/JCLI-D-11-00145.1>

Meinshausen, M., Nicholls, Z. R. J., Lewis, J., Gidden, M. J., Vogel, E., Freund, M., et al. (2020). The shared socio-economic pathway (SSP) greenhouse gas concentrations and their extensions to 2500. *Geoscientific Model Development*, 13(8), 3571–3605. <https://doi.org/10.5194/gmd-13-3571-2020>

Mindlin, J., Shepherd, T. G., Vera, C. S., Osman, M., Zappa, G., Lee, R. W., & Hodges, K. I. (2020). Storyline description of Southern Hemisphere midlatitude circulation and precipitation response to greenhouse gas forcing. *Climate Dynamics*, 54(9), 4399–4421. <https://doi.org/10.1007/s00382-020-05234-1>

Newman, M., Alexander, M. A., Ault, T. R., Cobb, K. M., Deser, C., Lorenzo, E. D., et al. (2016). The Pacific decadal oscillation, revisited. *Journal of Climate*, 29(12), 4399–4427. <https://doi.org/10.1175/JCLI-D-15-0508.1>

O'Reilly, C. H., Befort, D. J., Weisheimer, A., Woollings, T., Ballinger, A., & Hegerl, G. (2021). Projections of northern hemisphere extratropical climate underestimate internal variability and associated uncertainty. *Communications Earth & Environment*, 2(1), 1–9. <https://doi.org/10.1038/s43247-021-00268-7>

Ossó, A., Bladé, I., Karpechko, A., Li, C., Maraun, D., Romppainen-Martius, O., et al. (2024). Advancing our understanding of eddy-driven jet stream responses to climate change – a roadmap. *Current Climate Change Reports*, 11(1), 2. <https://doi.org/10.1007/s40641-024-00199-3>

Patterson, M., Bracegirdle, T., & Woollings, T. (2019). Southern hemisphere atmospheric blocking in CMIP5 and future changes in the Australia-New Zealand sector. *Geophysical Research Letters*, 46(15), 9281–9290. <https://doi.org/10.1029/2019GL083264>

Patterson, M., O'Reilly, C., Woollings, T., Weisheimer, A., & Wu, B. (2022). SST-driven variability of the East Asian summer jet on a decadal time-scale in CMIP6 models. *Quarterly Journal of the Royal Meteorological Society*, 148(743), 581–598. <https://doi.org/10.1002/qj.4219>

Poli, P., Hersbach, H., Dee, D. P., Berrisford, P., Simmons, A. J., Vitart, F., et al. (2016). ERA-20C: An atmospheric reanalysis of the twentieth century. *Journal of Climate*, 29(11), 4083–4097. <https://doi.org/10.1175/JCLI-D-15-0556.1>

Rayner, N. A., Parker, D. E., Horton, E. B., Folland, C. K., Alexander, L. V., Rowell, D. P., et al. (2003). Global analyses of sea surface temperature, sea ice, and night marine air temperature since the late nineteenth century. *Journal of Geophysical Research*, 108(D14). <https://doi.org/10.1029/2002JD002670>

Riviére, G. (2011). A dynamical interpretation of the poleward shift of the jet streams in global warming scenarios. *Journal of the Atmospheric Sciences*, 68(6), 1253–1272. <https://doi.org/10.1175/2011JAS3641.1>

Robertson, A. W. (1996). Interdecadal variability over the North Pacific in a multi-century climate simulation. *Climate Dynamics*, 12(4), 227–241. <https://doi.org/10.1007/BF00219498>

Rugenstein, M., Dhame, S., Olonscheck, D., Wills, R. J., Watanabe, M., & Seager, R. (2023). Connecting the SST pattern problem and the hot model problem. *Geophysical Research Letters*, 50(22), e2023GL105488. <https://doi.org/10.1029/2023GL105488>

Schneider, T. (2006). The general circulation of the atmosphere. *Annual Review of Earth and Planetary Sciences*, 34(34), 655–688. <https://doi.org/10.1146/annurev.earth.34.031405.125144>

Seager, R., Cane, M., Henderson, N., Lee, D.-E., Abernathey, R., & Zhang, H. (2019). Strengthening tropical Pacific zonal sea surface temperature gradient consistent with rising greenhouse gases. *Nature Climate Change*, 9(7), 517–522. <https://doi.org/10.1038/s41558-019-0505-x>

Seager, R., Henderson, N., & Cane, M. (2022). Persistent discrepancies between observed and modeled trends in the tropical Pacific Ocean. *Journal of Climate*, 35(14), 4571–4584. <https://doi.org/10.1175/JCLI-D-21-0648.1>

Shaw, T. A. (2019). Mechanisms of future predicted changes in the zonal mean mid-latitude circulation. *Current Climate Change Reports*, 5(4), 345–357. <https://doi.org/10.1007/s40641-019-00145-8>

Simpson, I. R., Deser, C., McKinnon, K. A., & Barnes, E. A. (2018). Modeled and observed multidecadal variability in the North Atlantic jet stream and its connection to sea surface temperatures. *Journal of Climate*, 31(20), 8313–8338. <https://doi.org/10.1175/JCLI-D-18-0168.1>

Simpson, I. R., Shaw, T. A., & Seager, R. (2014). A diagnosis of the seasonally and longitudinally varying midlatitude circulation response to global warming. *Journal of Climate*, 27(7), 2489–2515. <https://doi.org/10.1175/JCLI-D-13-0325.1>

Slivinski, L. (2019). Noaa-cires-doe twentieth century reanalysis version 3. *Research Data Archive at the National Center for Atmospheric Research, Computational and Information Systems Laboratory*. [Dataset]. <https://doi.org/10.5065/D6VQ30QG>

Slivinski, L. C., Compo, G. P., Sardeshmukh, P. D., Whitaker, J. S., McColl, C., Allan, R. J., et al. (2021). An evaluation of the performance of the twentieth century reanalysis version 3. *Journal of Climate*, 34(4), 1417–1438. <https://doi.org/10.1175/JCLI-D-20-0505.1>

Titchner, H. A., & Rayner, N. A. (2014). The Met Office hadley Centre sea ice and sea surface temperature data set, version 2: 1. Sea ice concentrations. *Journal of Geophysical Research: Atmospheres*, 119(6), 2864–2889. <https://doi.org/10.1002/2013JD020316>

Trenberth, K. E., Branstator, G. W., Karoly, D., Kumar, A., Lau, N.-C., & Ropelewski, C. (1998). Progress during TOGA in understanding and modeling global teleconnections associated with tropical sea surface temperatures. *Journal of Geophysical Research*, 103(C7), 14291–14324. <https://doi.org/10.1029/97JC01444>

Trenberth, K. E., & Hurrell, J. W. (1994). Decadal atmosphere-ocean variations in the Pacific. *Climate Dynamics*, 9(6), 303–319. <https://doi.org/10.1007/BF00204745>

Watanabe, M., Dufresne, J.-L., Kosaka, Y., Mauritsen, T., & Tatebe, H. (2021). Enhanced warming constrained by past trends in equatorial Pacific sea surface temperature gradient. *Nature Climate Change*, 11(1), 33–37. <https://doi.org/10.1038/s41558-020-00933-3>

Williams, N. C., Scaife, A. A., & Screen, J. A. (2023). Underpredicted ENSO teleconnections in seasonal forecasts. *Geophysical Research Letters*, 50(5), e2022GL101689. <https://doi.org/10.1029/2022GL101689>

Wills, R. C. J., Dong, Y., Proistosecu, C., Armour, K. C., & Battisti, D. S. (2022). Systematic climate model biases in the large-scale patterns of recent sea-surface temperature and sea-level pressure change. *Geophysical Research Letters*, 49(17), e2022GL100011. <https://doi.org/10.1029/2022GL100011>

Woolings, T., Drouard, M., O'Reilly, C. H., Sexton, D. M. H., & McSweeney, C. (2023). Trends in the atmospheric jet streams are emerging in observations and could be linked to tropical warming. *Communications Earth & Environment*, 4(1), 1–8. <https://doi.org/10.1038/s43247-023-00792-8>

Woolings, T., Hannachi, A., & Hoskins, B. (2010). Variability of the North Atlantic eddy-driven jet stream. *Quarterly Journal of the Royal Meteorological Society*, 136(649), 856–868. <https://doi.org/10.1002/qj.625>

Wu, M., Zhou, T., Li, C., Li, H., Chen, X., Wu, B., et al. (2021). A very likely weakening of Pacific Walker Circulation in constrained near-future projections. *Nature Communications*, 12(1), 6502. <https://doi.org/10.1038/s41467-021-26693-y>

Zappa, G., Pithan, F., & Shepherd, T. G. (2018). Multimodel evidence for an atmospheric circulation response to Arctic sea ice loss in the CMIP5 future projections. *Geophysical Research Letters*, 45(2), 1011–1019. <https://doi.org/10.1002/2017GL076096>

Zappa, G., & Shepherd, T. G. (2017). Storylines of atmospheric circulation change for European regional climate impact assessment. *Journal of Climate*, 30(16), 6561–6577. <https://doi.org/10.1175/JCLI-D-16-0807.1>

Zhang, R., Sutton, R., Danabasoglu, G., Kwon, Y.-O., Marsh, R., Yeager, S. G., et al. (2019). A review of the role of the Atlantic meridional overturning circulation in Atlantic multidecadal variability and associated climate impacts. *Reviews of Geophysics*, 57(2), 316–375. <https://doi.org/10.1029/2019RG000644>